In Silico Analysis and Optimization of Multi-Epitope mRNA Vaccine Candidates Derived from the Proteome of *Toxocara canis*

Roohollah Fattahi [1]✉ iD

[1] Department of laboratory and clinical sciences, Faculty of veterinary sciences, Ilam University,Ilam,Iran

Article Info	A B S T R A C T
Article type: Original Article	**Introduction**: *Toxocara canis* is a significant zoonotic parasite that remains inadequately controlled. This study utilized a range of immunoinformatics methodologies to develop a candidate multi-epitope mRNA vaccine against *T. canis*.
	Materials & Methods: From a total of 39,233 proteins catalogued in the NCBI database for *T. canis*, eleven highly antigenic proteins were carefully selected using various software and server tools, and their epitopes were identified through advanced immunoinformatics techniques. Then, the selected epitopes underwent thorough evaluation for their biological characteristics and homology. Furthermore, the presentation of these epitopes by MHC cells and other immune cells was analysed using molecular docking approaches. A multi-epitope protein was subsequently modelled and improved, followed by an extensive structural and stability analysis of the vaccine candidate. The immune response triggered by this innovative vaccine was simulated and analysed.
✉ *Correspondence to:* Roohollah Fattahi Department of laboratory and clinical sciences, Faculty of veterinary sciences, Ilam University,Ilam,Iran **Email:** r.fattahi@ilam.ac.ir	**Results:** The findings demonstrated that the developed vaccine possessed antigenic characteristics, was basic in nature, and showed no toxicity or allergenic potential. Notably, the identified epitopes were localised within the antigen-binding sites of their corresponding MHC alleles. The immune simulation revealed elevated levels of immunoglobulins, T helper cells, cytotoxic T cells, and activated natural killer (NK) cells, macrophages, and dendritic cells, along with significant cytokine production. Additionally, molecular dynamics simulations revealed strong and stable interactions with Toll-like receptors, specifically TLR2, TLR3, and TLR4.
	Conclusion: Computational immune simulation studies demonstrated a notable increase in immune reactivity towards the developed vaccine. Given these results, the proposed vaccine candidate shows strong potential and is ready for additional evaluation as an innovative mRNA-based therapeutic approach to combat toxocariasis.

➤ **Cite this paper**

Fattahi R. In Silico Analysis and Optimization of Multi-Epitope mRNA Vaccine Candidates Derived from the Proteome of *Toxocara canis*. *J Bas Res Med Sci*. 2026; 13(1):43-66.

Introduction

Toxocariasis is caused mainly by *T. canis* in dogs and to a lesser extent by T. cati in cats. This disease is a common infection between humans and canids with a global distribution. Toxocariasis has been comprehensively overlooked. The natural hosts are canids, which are highly susceptible to *T. canis* infections. On the other hand, some vertebrate species, such as humans, play a role as incidental hosts (1). *Toxocara canis* has a complex life cycle with multiple stages and hosts, which allow it to persist and be transmitted in different environments. Moreover, the complexity of the parasite's life cycle presents serious challenges for the prevention and control of toxocariasis, especially in areas where human-carnivore interactions are high (1, 2). Especially, eggs produced by adult worms in the dog's intestines are shed to the environment through faeces. Notably, these released eggs are very resistant and remain viable and infectious for a long time in water, soil, and various surfaces. Subsequently, when dogs ingest these larval eggs, large numbers of second-stage larvae migrate into their small intestines. There, they mature and after mating, the females produce eggs (1). Meanwhile, humans are infected by accidentally ingesting these eggs, including by touching contaminated surfaces (3). Additionally, vertical transmission has been reported in humans and also in dogs (4). However, these larvae do not mature in the human intestine but rather pass through the intestinal wall and enter the bloodstream, reaching various tissues and forming cysts as second-stage larvae (3, 5). In general, human infection with *Toxocara canis* larvae is mostly asymptomatic. However, the occurrence of clinical symptoms depends on factors such as the severity of the infection and the host's inflammatory response severity. Additionally, humans Toxocariasis has four clinical forms, including visceral larva migrants (VLM), ocular larva migrants (OLM), neurological larva migrants (NLM), and covert or asymptomatic toxocariasis (6). Furthermore, identifying high-risk populations and implementing effective prevention

strategies against Toxocariasis depend on understanding the epidemiology of this disease (7, 8). To date, no completely effective vaccine has been developed to prevent toxocariasis. One of the key reasons is the parasite's complex mechanisms for evading the host's immune system, which pose a significant challenge for the lack of an effective vaccine. As an example, this parasite effectively modulates the immune response by producing some secretory-excretory substances and provides a suitable environment to survive in the host's body (8). Furthermore, *Toxocara* eggs are highly persistent in the environment and have the potential for reinfection, so a vaccine must not only be effective but also provide long-term immunity. Another problem is that cyst formation by second-stage larvae in various human tissues can result in larval persistence without eliciting significant inflammatory responses. These obstacles highlight the importance of innovative approaches in vaccine development (9). Introducing an effective vaccine against *Toxocara* could be very beneficial for humans and dogs because it not only prevents infection in these hosts but also helps reduce environmental contamination and subsequent transmission to humans (6). Recent advances in vaccine development for multicellular organisms, including helminths, could make such vaccines possible. Research involving recombinant antigens has shown remarkable effectiveness, providing 90-100% protection against infections from Taenia ovis in sheep, Taenia solium in cattle, and Echinococcus granulosus in sheep. These advancements highlight the potential of using molecular biology approaches to develop a vaccine for toxocariasis, offering significant benefits for both veterinary and human health (6, 8, 10, 11). Bioinformatics tools are now widely used by scientists in biotechnology and immunology to predict antigenic epitopes. By analysing accessibility and antigenicity, this computational approach improves the accuracy of identifying epitopes. Furthermore, the design and construction of multi-epitope recombinant antigens based on these predicted epitopes offers a promising

avenue for the development of cost-effective vaccines (8, 12, 13). Based on the preceding statements, this research focuses on designing an innovative multi-epitope mRNA vaccine incorporating cytotoxic T lymphocyte (CTL), helper T lymphocyte (HTL), and linear B lymphocyte (LBL) epitopes sourced from the antigenic proteins of *T. canis*.

Materials and methods

Retrieval of protein sequences

1. Collection of Protein Sequences

The amino acid sequences of *T. canis* were retrieved from the NCBI database to perform a comprehensive analysis of their structural and functional features. First, sequences with signal peptides were detected using the SignalP 6.0 server (28). This server identifies the existence and position of signal peptide sequences within proteins.

2. Prediction of Subcellular Localisation

To predict the locations of proteins within cells, the DeepLoc-2.1 server (29) was used. This server predicts the subcellular localisation of proteins inside cells. Additionally, the TMHMM server was applied to predict the cell wall proteins, which is useful for predicting transmembrane helices in proteins. Moreover, the potential of proteins with signal peptides to trigger an immune response was evaluated using the Vaxijen server (30). Finally, the proteins exhibiting the highest levels of antigenicity, particularly those associated with the cell membrane and extracellular environments, were selected for the final vaccine design.

Prediction of immune cell epitopes

1. Prediction of LBL epitopes

The ABCpred server (31) was utilized to identify potential LBL epitopes; this tool relies on an artificial neural network to predict potential B-cell epitopes. The server was programmed to analyse peptides of a fixed length of 16 amino acids, resulting in an 80% specificity. Additionally, to enhance prediction accuracy, an overlap filter was activated, and a threshold of 0.8 was applied to the protein sequences.

2. Prediction of CTL and HTL epitopes

CTL epitopes were predicted by the IEDB MHC I web server (32), according to the prescribed method. The netMHCpan 4.1 EL setting was used to predict CTL epitopes with lengths of 9-10 amino acids. For this purpose, the selected proteins in FASTA format were analysed using a comprehensive set of human HLA and dog DLA alleles. Finally, the predicted epitopes were ranked based on their IC50 values to determine their binding strength. Furthermore, in order to predict HTL epitopes, the IEDB MHC-II server was used. The NetMHCIIpan 4.1 EL setting was also used to predict HTL epitopes with a length of 16 amino acids (33). Ultimately, the CTL and HTL epitopes with the strongest antigenic characteristics were selected for the final vaccine construct to enhance immune recognition and response.

Human and dog Homology

In order to avoid cross-reactivity, all selected epitopes were screened against the proteomes of Homo sapiens (TaxID: 9606) and Canis lupus (dog, TaxID: 9615) using the BLASTP tool in the NCBI database. Epitopes homologous to humans with an E-value below 0.05 were excluded and the epitopes with an E-value greater than 0.05 were considered as non-homologous. These remaining non-homologous epitopes were selected for further analysis.

Prediction of epitope's antigenicity, allergenicity and toxicity

1. Epitope's antigenicity, allergenicity and toxicity

Antigenicity, allergenicity, and toxicity of the selected epitopes were evaluated using several bioinformatics servers. The Vaxijen server was used to assess the antigenicity of the selected epitopes (threshold of 0.7). Additionally, we used the AlgPred

v.2.0 web server with a threshold of 0.4 to predict the allergenicity of selected epitopes (34). Also, for evaluating the potential toxicity of selected epitopes, the ToxinPred server was used with its default parameters (35). Finally, we select epitopes with strong antigenic potential that are devoid of toxicity and allergenicity for further study in our research.

2. Cytokine induction

The HTL epitopes were tested for their potential to induce key cytokines, particularly interferon-gamma (IFN-γ), interleukin-4 (IL-4), interleukin-6 (IL-6), and interleukin-17 (IL-17). This assessment was done using various advanced tools such as IFNepitope (36), IL4pred (37), IL6pred (38), IL10pred (39), and IL13pred (40).

Molecular docking between T cell epitopes and their corresponding MHC alleles

To determine the binding affinity of specific T-lymphocyte epitopes with their corresponding major histocompatibility complex (MHC) alleles, we used the ClusPro 2.0 server for molecular docking analysis. We obtained the 3D structures of these corresponding MHC alleles from the RCSB Protein Data Bank (PDB) and then refined them using PyMOL software to eliminate unnecessary ligands. To ensure optimal structural integrity, we conducted energy minimisation using Swiss-PDB Viewer (41). The PEP-FOLD 3.5 server (42) was used to build the 3D structures of the selected T-lymphocyte epitopes, and then their energy was minimised using Swiss-PDB Viewer before docking. Finally, docking was performed using the ClusPro 2.0 server.

Design of the Vaccine Construct

The CTL, HTL, and LBL epitopes, which exhibit high antigenicity, low allergenicity, and minimal toxicity, were linked together using AAY, GPGPG, and KK, respectively. The vaccine construct begins with a modified cap structure (m7GCap), followed by a 5' untranslated region (5'UTR) and a Kozak sequence to enhance translation efficiency. The

coding region is initiated by a signal peptide (tPA), which is linked to an adjuvant component (RpfE) through an EAAAK linker. Adjuvants are crucial in vaccine constructs for effectively activating innate immunity and eliciting an immune response. Our selected epitopes were placed next, followed by the MITD sequence, a stop codon, a 3' untranslated region (3'UTR), and a poly(A) tail, which were added to the mRNA vaccine construct (43).

Assessment of Antigenicity, Allergenicity, Toxicity, and Physicochemical Properties of the Vaccine construct

The antigenicity, allergenicity, and toxicity of the vaccine construct were evaluated using the VaxiJen 2.0, AlgPred 2.0, and ToxinPred online tools, respectively. These analyses focused on the selected epitopes and their linkers within the mRNA vaccine. Additionally, various physicochemical characteristics, including amino acid composition, molecular weight, theoretical isoelectric point (pI), instability index (II), aliphatic index (A.I.), and grand average of hydropathicity (GRAVY), were evaluated through the ProtParam web server (44).

In Silico Immune Simulation

In silico immune simulations were conducted using the C-ImmSim server (45) to predict immunological responses to the mRNA vaccine (all epitopes and their linkers). These simulations involved administering three doses of 1000 vaccine units over four weeks, with all parameters set to default and injections scheduled at intervals of 1, 84, and 168 hours.

Codon Optimisation

Codon optimization of the mRNA vaccine construct was performed using the Java Codon Adaptation Tool (JCat) server (46). The quality of the optimised sequence was evaluated through Rare Codon Analysis tools, and translation efficiency was assessed via the Codon Adaptation Index (CAI).

Secondary Structure Prediction

The secondary structure of the mRNA vaccine construct was analysed using RNAfold from the Vienna RNA Package 2.0, which calculated the minimum free energy (MFE) of the predicted structure. This analysis provided insights into both the MFE structure and centroid secondary structure (47).

Secondary and Tertiary Structure Prediction

For predicting secondary structures of peptide sequences in the mRNA vaccine construct, including selected CTL, HTL and LBL epitopes along with their linkers, the PSIPRED server was used (48). Subsequently, the structure was submitted to the Alphafold 2 server for three-dimensional homology modelling (49). AlphaFold 2 uses advanced deep learning methods, working with multiple sequence alignments (MSA) and evolutionary data, to predict protein 3D structures. It analyses the amino acid sequence and relies on a detailed neural network that identifies connections between residues, repeatedly improving the predicted structures for better accuracy. Finally, the optimal model achieved by the Alphafold 2 server was validated using ProSA-web (50), PROCHECK (51), and ERRAT. ProSA-web checks structural quality by analysing energy profiles, while PROCHECK verifies proper folding and geometry by assessing stereochemical parameters. ERRAT further examines the non-bonded interactions within the model, providing additional insights into its structural integrity and reliability (50).

Conformational B-cell Epitope Prediction

Conformational B-cell epitopes were identified using the ElliPro online server, which employs geometric properties from 3D models for epitope prediction. Notably, ElliPro exhibited superior performance with an AUC value of 0.732 compared to other tools (52).

Molecular Docking between mRNA vaccine construct and Toll-like receptors (TLRs)

The ClusPro server was used to analyse the interactions between our mRNA vaccine construct and TLR2 (PDB ID: 2Z7X), TLR3 (PDB ID: 7c76) and TLR4 (PDB ID: 2z63). This computational server uses docking algorithms to predict binding affinities and structural orientations between the vaccine construct and TLRs. Also, it shows the binding strength and position of the vaccine construct and its related TLRs to help elucidate immune responses. Furthermore, PyMOL was utilized to visualise the docking complexes effectively. Additionally, LigPlot was employed to identify the interacting residues between the vaccine construct and the immunoreceptors (53).

Molecular Dynamics Simulation

To confirm the atomic and molecular dynamics within the TLR2-vaccine, TLR3-vaccine and TLR4-vaccine complex structures, dynamic simulation analyses were performed using the iMODS server (54). Furthermore, iMODS allows us to explore the normal modes of motion, giving researchers a visual representation of potential conformational changes that might occur during the intricate dance of ligand-receptor interactions.

Results

Acquisition of protein sequences

In this study, the NCBI database was searched for protein sequences related to *T. canis*, and a total of 39,233 sequences were retrieved in FASTA format. Of these, 2,622 proteins were identified as containing signal peptides using the SignalP 6.0 server. Analysis using the DeepLoc 2.1 and TMHMM servers showed that among the 2,622 proteins, 1,745 (66.55%) were assigned as extracellular (secreted) proteins, 466 (17.77%) as cell membrane proteins, 124 (4.20%) as cytoplasmic proteins, 170 (6.48%) as endoplasmic reticulum proteins, and 117 (4.46%) as other cellular locations. For further investigation, both the extracellular and cell membrane proteins were submitted to the Vaxijen v2 server (with a threshold of 0.9) to assess their antigenic properties. From a

total of 2,211 proteins analysed, 82 exhibited antigenicity scores exceeding 0.9. Finally, from these 82 highly antigenic proteins, we selected 11 (6 extracellular and 5 cell membrane proteins) for the vaccine construct based on their immune response potential. The accession numbers of the 11 selected proteins are as follows: KHN86360.1 - KHN85124.1 - KHN82102.1 - KHN81097.1 - KHN76331.1 - KHN73223.1 - KHN72223.1 - VDM40353.1 - VDM41926.1 - VDM45745.1 - VDM46706.1 (Table 1).

Immune Cell Epitope Prediction and Validation

In this research, the specialised servers were used to predict and validate various epitopes essential for

vaccine development. A total of 44 epitopes were selected from 11 proteins, including 22 CTL epitopes, 11 HTL epitopes, and 11 B cell epitopes, with each protein providing two CTL epitopes, one HTL epitope, and one B cell epitope. All chosen epitopes demonstrated strong antigenic properties, were non-allergenic and non-toxic, and showed no similarity to proteins present in humans or dogs. Detailed information regarding these selected epitopes is presented in Table 1. Additionally, all selected helper T lymphocytes (HTLs) epitopes induced interleukin IL-5 and IL-10, while nine of the HTLs epitopes also stimulated the production of IL-4. Furthermore, three HTLs were found to induce interferon (IFN), and one HTL induced IL-13. Detailed information is presented in Table 2.

Table 1. The final CTL, HTL, and LBL epitopes incorporated into the vaccine design.

Protein ID	Function	localization	CTL epitopes	MHC I binding alleles	Th2	MHC2 binding alleles	B cell epitopes
>KHN86360.1	hypothetical protein Tcan_13999 [*Toxocara canis*]	Cell membrane	SLNNNMHNV	HLA-A*02:03 DLA-8850101	SASNVSIFK RKKRDV	HLA-DRB1*13:02	DAKIDASG GGNANVNS
			VIANQTLTW	HLA-B*58:01 DLA-8803401			
>KHN85124.1	hypothetical protein Tcan_10097 [*Toxocara canis*]	Cell membrane	YSDYSGGGY	HLA-A*01:01 DLA-8803401	GHNGYTAS SGYPDTS	HLA-DRB1*09:01	SGSGISRPY DGNGHAP
			MPKVPSTSF	HLA-B*07:02 DLA-8803401			
>KHN82102.1	Paternally-expressed protein [*Toxocara canis*]	Cell membrane	SESPPTAVL	HLA-B*40:01 DLA-8850801	EESFMQST ASKLESI	HLA-DRB1*09:01	SFSIDEPTE DSNKENA
			ESDNCTLYY	HLA-A*01:01 DLA-8850801			
>KHN81097.1	Circumsporozoite protein [*Toxocara canis*]	Extracellular	ETNFGHVRYR	HLA-A*68:01 DLA-8803401	FGHVRYRK RYRYRKP	HLA-DRB1*13:02	HVRYRKRY RYRKPQTT
			QSRYGQRPYW	HLA-B*57:01 DLA-8803401			
>KHN76331.1	Transthyretin-like protein 5 [*Toxocara canis*]	Extracellular	TTIDPKLNVY	HLA-A*01:01 DLA-8850101	NVKVKLY DDDRGVD A	HLA-DQA1*01:01 /DQB1*05:0 1	YHDCEDAL TPCQRKIT
			KLYDDDRGV	HLA-A*02:03 DLA-8850801			
>KHN73223.1	hypothetical protein Tcan_11988, partial	Cell membrane	TPHSRGNAM	HLA-B*07:02 DLA-8803401	CRQLFDDS IYSSLPE	HLA-DPA1*01:03 /DPB1*04:01	QQQQRTPG TPHSRGNA
			SIYSSLPEV	HLA-A*02:06 DLA-8850101			

	[*Toxocara canis*]						
>KHN72223.1	Collagen alpha-1(IV) chain [*Toxocara canis*]	Extracellular	SEQISLRGF	HLA-B*44:03 DLA-8803401	DGPPGYVG LKGQKGD	HLA-DRB1*01:01	FPGPQGPK GRMGIRTP
			TPLPVTIIV	HLA-B*51:01 DLA-8850101			
>VDM40353.1	unnamed protein product [*Toxocara canis*]	Extracellular	YPQRGAPAY	HLA-B*35:01 DLA-8803401	LSRYLKDS TLHSKKK	HLA-DRB1*04:01	AASGYEYP QRGAPAYD
			YPSYPSDAY	HLA-B*35:01 DLA-8803401			
>VDM41926.1	unnamed protein product [*Toxocara canis*]	Extracellular	HEMDSIKMM	HLA-B*44:03 DLA-8803401	ASGRVGEP GARGKAG	HLA-DPA1*02:01 /DPB1*14:01 1	RGMRGAA GRPGYPGN D
			RVGEPGARGK	HLA-A*03:01 DLA-8850101			
>VDM45745.1	unnamed protein product [*Toxocara canis*]	Extracellular	APSGPGPAM	HLA-B*07:02 DLA-8803401	YRASFRTV AAVRRRV	HLA-DRB5*01:01	HVAKVSRP TSNSIVDN
			AMLPPPPTR	HLA-B*15:01 DLA-8850801			
>VDM46706.1	unnamed protein product [*Toxocara canis*]	Extracellular	HSSRVRVKR	HLA-B*57:01 DLA-8850801	AQPIEAHSS RVRVKR	HLA-DRB1*13:02	GGLGGSHG LHAIVVSP
			HAIVVSPHGW	HLA-B*57:01 DLA-8850801			

Table 2. Selected HTL epitopes along with their associated cytokine induction capabilities.

HTL epitope	IL4	IL5	IL10	IL13	IFN
SASNVSIFKRKKRDV	inducer	inducer	inducer	non-inducer	Positive
GHNGYTASSGYPDTS	Non-inducer	inducer	inducer	non-inducer	negative
EESFMQSTASKLESI	inducer	inducer	inducer	non-inducer	negative
FGHVRYRKRYRYRKP	inducer	inducer	inducer	inducer	positive
NVKVKLYDDDRGVDA	inducer	inducer	inducer	non-inducer	negative
CRQLFDDSIYSSLPE	inducer	inducer	inducer	non-inducer	negative
DGPPGYVGLKGQKGD	Non-inducer	inducer	inducer	non-inducer	negative
LSRYLKDSTLHSKKK	inducer	inducer	inducer	non-inducer	positive
ASGRVGEPGARGKAG	inducer	inducer	inducer	non-inducer	negative
YRASFRTVAAVRRRV	inducer	inducer	inducer	non-inducer	negative
AQPIEAHSSRVRVKR	inducer	inducer	inducer	non-inducer	negative

Molecular docking analysis of T-lymphocyte epitopes with MHC alleles

All 22 CTL epitopes were docked with their corresponding HLA MHC-I alleles, as well as with the DLA-MHC-I alleles of dogs. Among these, the predicted CTL epitopes HAIVVSPHGW, ESDNCTLYY, QSRYGQRPYW, VIANQTLTW, and ETNFGHVRYR demonstrated the highest binding affinities to their human MHC-I alleles, exhibiting energy values of -1102.8, -853.0, -851.0, -832.5, and -827.6 kcal/mol, respectively. Similarly, the epitopes HAIVVSPHGW, VIANQTLTW, QSRYGQRPYW, ESDNCTLYY, and AMLPPPPTR showed strong binding affinities with their corresponding dog MHC-I alleles, with energy values of -1013.4, -887.7, -840.3, -799.6, and -790.8 kcal/mol, respectively (Table 3). Additionally, the identified helper T cell epitopes were analysed through molecular docking with their respective human MHC-II alleles. Among these, the predicted HTL epitopes YRASFRTVAAVRRRV, FGHVRYRKRYRYRKP, NVKVKLYDDDRGVDA and

AQPIEAHSSRVRVKR showed the highest binding affinities to their human MHC-II alleles; some results are presented in Table 3. Figures 1 and 2 illustrate several robust binding models of CTL epitopes interacting with both human and dog MHC-I alleles, as well as HTL epitopes with human MHC-II alleles. Finally, the interactions between the predicted epitopes and their corresponding MHC alleles were evaluated using the LigPlot+ tool, as illustrated in Figures 1 and 2.
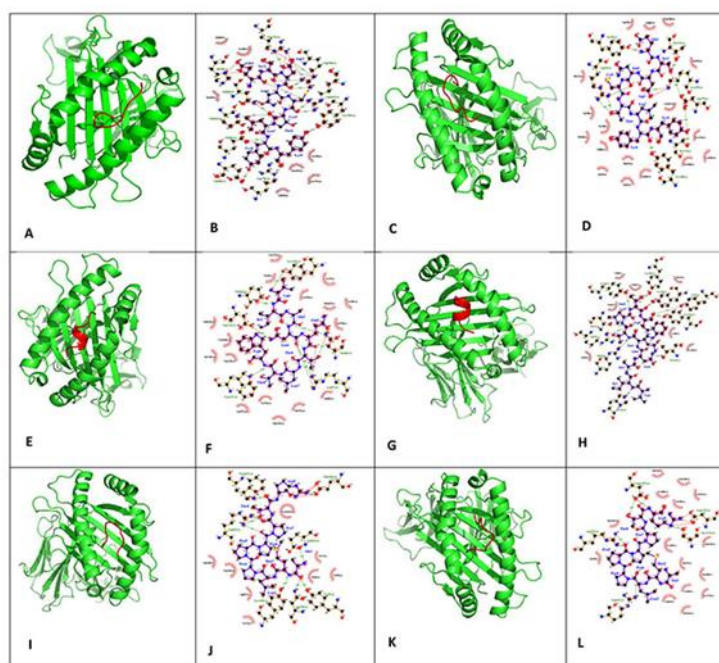

Figure 1. Docking and interactions between selected CTL epitopes and their respective MHC-I alleles using ClusPro 0.2 and LigPlot+. A, B; docking and interaction between HLA-A*01:01 allele and ESDNCTLYY, respectively. C and D; docking and interaction between DLA-8850801 allele and ESDNCTLYY, respectively. E, F; docking and interaction between HLA-B*58:01 allele and VIANQTLTW, respectively.G, H; docking and interaction between DLA-8803401 allele and VIANQTLTW, respectively.I, J; docking and interaction between HLA-B*15:01 allele and AMLPPPPTR, respectively.K, L; docking and interaction between DLA-8850801 allele and AMLPPPPTR, respectively.
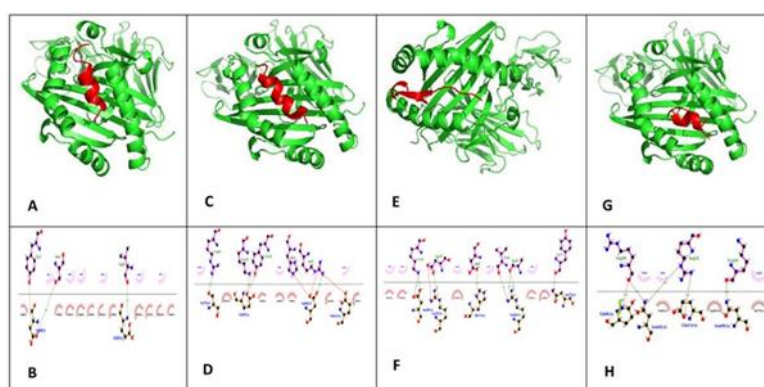

Figure 2. Docking and interactions between some selected HTL epitopes and their respective MHC-II alleles. A, B; docking and interaction between HLA-DRB5 allele and YRASFRTVAAVRRRV, respectively. C, D; docking and interaction between HLA-DRB1 allele and FGHVRYRKRYRYRKP, respectively. E, F; docking and interaction between HLA-DQA1 allele and NVKVKLYDDDRGVDA, respectively. G, H; docking and interaction between HLA-DRB1 allele and AQPIEAHSSRVRVKR, respectively.

Table 3. Docking analysis of some selected CTL and HTL epitopes along with their binding affinity energies to corresponding MHC alleles.

Type of T lymphocyte	Epitope	MHC alleles	RCSB ID of MHC allele	Binding affinity (kcal/mol)
CTL	HAIVVSPHGW	HLA-B*57:01	5vuf	-1102.8
		DLA-8850801	5F1N	-1013.4
	ESDNCTLYY	HLA-A*01:01	4nqx	-853.0
		DLA-8850801	5F1N	-799.6
	QSRYGQRPYW	HLA-B*57:01	5vuf	-851.0
		DLA-8803401	7CJQ	-840.3
	VIANQTLTW	HLA-B*58:01	5vwh	-832.5
		DLA-8803401	7CJQ	-887.7
	ETNFGHVRYR	HLA-A*68:01	6pbh	-827.6
	AMLPPPPTR	DLA-8850801	5F1N	-790.8
HTL	YRASFRTVAAVRRRV	HLA-DRB5	1H15	-895.8
	FGHVRYRKRYRYRKP	HLA-DRB1	6atz	-880.7
	NVKVKLYDDDRGVDA	HLA-DQA1	6dig	-843.3
	AQPIEAHSSRVRVKR	HLA-DRB1	6atz	-803.4
	CRQLFDDSIYSSLPE	HLA-DPA1	7zfr	-742.8
	SASNVSIFKRKKRDV	HLA-DRB1	6atz	-723.1

Development of the Vaccine Construct

The final design of our mRNA vaccine comprises the following elements: a 5' m7G cap, 5' UTR, Kozak sequence, a signal peptide (tPA), an EAAAK Linker, Adjuvant (RpfE), an AAY linker, 22 CTL epitopes (with an AAY linker between them), 11 HTL epitopes (with a GPGPG linker between them) and 22 LBL epitopes (with a KK linker between them) and in the N-terminus, an MITD sequence–Stop codon–3'UTR and Poly(A) tail were added, respectively (Figure 3).

Figure 3. Assembly of the candidate mRNA vaccine is depicted, with distinct linkers facilitating the connections between various epitopes. The red lines represent AAY linkers that connect CTL epitopes, while the green lines denote GPGPG linkers linking HTL epitopes. Additionally, the yellow lines illustrate KK linkers that associate with B cell epitopes.

Evaluation of Antigenicity, Allergenicity, Toxicity, and Physicochemical Characteristics of the Final Vaccine Design

The findings of this study indicated that the vaccine construct demonstrated notable antigenic properties, as reflected by a VaxiJen score of 0.7197 and an ANTIGENpro score of 0.8762. Furthermore, analyses conducted with the AlgPred and ToxinPred servers verified that the vaccine is both non-allergenic and non-toxic. Notably, according to the ProtParam server, the vaccine peptide consists of 687 amino acids and has a molecular weight of 73,508.36 Daltons. The predicted half-life of this vaccine construct varies significantly across different environments: approximately 1.9 hours in mammalian reticulocytes (in vitro), over 20 hours in yeast (in vivo), and more than 10 hours in Escherichia coli (in vivo). Moreover, an instability index of 34.71 suggests favourable stability for the vaccine. The aliphatic index, measured at 49.42, classifies the vaccine as a thermostable protein. The theoretical isoelectric point (pI) was 9.92, and the GRAVY index

of -0.800 indicates a polar nature with strong water interaction, implying high solubility. Additionally, the analysis showed that the number of negatively charged residues (Asp + Glu) was 47, while positively charged residues (Arg + Lys) totalled 101. The chemical formula for the vaccine was identified as $C_{3253}H_{5010}N_{966}O_{961}S_{15}$ (Table 4). As illustrated in Figure 4, The solubility of the vaccine construct, represented by the QuerySol scaled solubility value, was calculated to be 0.523. Collectively, these findings suggest that the mRNA vaccine construct developed in this study holds significant promise as an effective candidate against *T. canis*.

Table 4. The various physicochemical characteristics of the finalized vaccine construct.

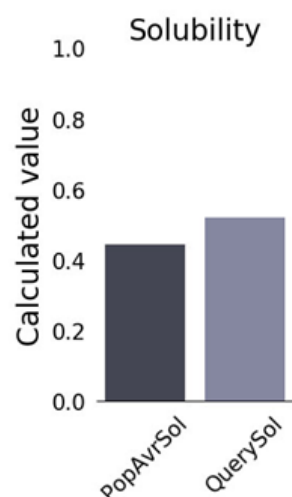| Property	Measurement	Indication
Total number of amino acids	687	Appropriate
Molecular weight	73508.36 Da	Appropriate
Formula	$C_{3253}H_{5010}N_{966}O_{961}S_{15}$	–
Theoretical pI	9.92	base
Total number of negatively charged residues (Asp + Glu)	47	–
Total number of positively charged residues (Arg + Lys)	101	–
Total number of atoms	10205	–
Instability Index (II)	34.71	Stable
Aliphatic Index (A.I.)	49.42	Thermostable
Grand average of hydropathicity (GRAVY)	-0.800	Hydrophilic
Antigenicity (using VaxiJen)	0.7197	Antigenic
Antigenicity (using ANTIGENpro)	0.876271	Antigenic
Allergenicity (using AllerTop 2.0)	Non-allergenic	Non-allergenic
Toxicity (ToxinPred)	Non-toxic	Non-toxic

Figure 4. Solubility of the vaccine construct as determined by QuerySol, showing a solubility score of 0.523

Computational Simulation of Immune Response to the Designed Vaccine

The results from C-ImmSim highlight the strong and efficient induction of immunity. Notably, the data demonstrate that our vaccine construct is capable of activating and enhancing the function of natural killer (NK) cells, macrophages, and dendritic cells. Notably, we observed an increase in various cell types. These factors are crucial for promoting an

efficient immune response, which peaks on the days of application. Our findings showed that the vaccine construct effectively enhanced T helper cells, especially Th1. Th1 cells have an important effect on promoting cytotoxic T lymphocyte (CTL) expansion and strengthening cytotoxic responses. Furthermore, the population of active cytotoxic T lymphocytes increased on day 7 and remained elevated. Additionally, CTL and HTL levels increased with associated memory generation. In addition to this stimulation of T helper cells, our vaccine construct appears to enhance the production of IFN-γ, TGF-b, IL10, IL12 and IL2; they are critical cytokines for the immune response against different pathogens.

Another key finding was the rise in active cytotoxic cells coupled with a decline in resting cytotoxic cells, both of which are critical for managing parasitic infections. Computational simulations of the proposed vaccine administration showed a growth in the memory B cell population during the injection period, with a significant shift towards memory B cell specialisation and a concurrent reduction in non-memory B cells. Additionally, during the injection phases, we observed a substantial increase in antibody generation, including IgM + IgG, IgG1, and IgG1 + IgG2. Furthermore, macrophage and dendritic cell activity was elevated, while epithelial activity remained stable (Figure 5).
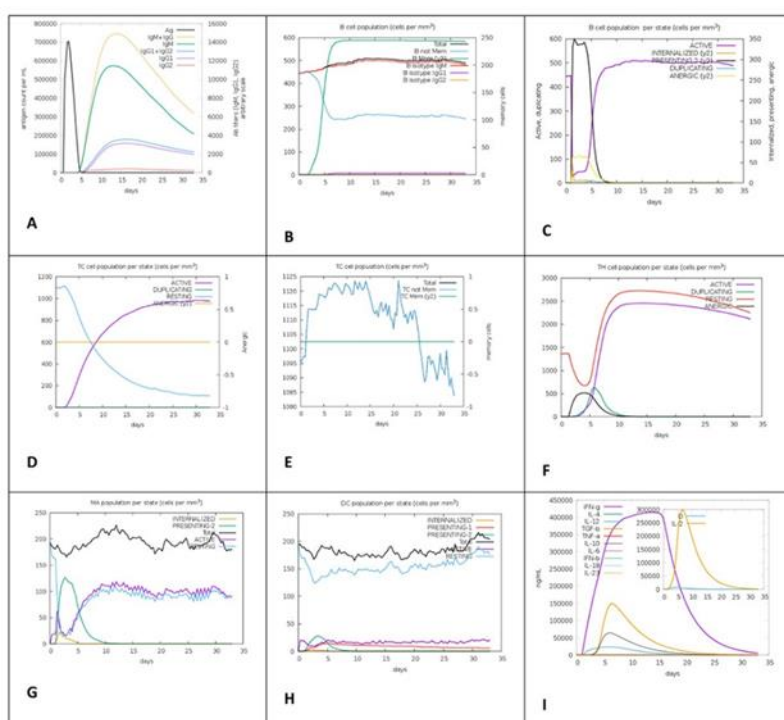

Figure 5. In silico Simulation of the immune response to the mRNA vaccine conducted using the C-ImmSim server. (A) The antibody production. (B) The B-cell population. (C) The B-cell population. (D) T-cell population. (E) T-cell population. (F) The helper Tcell population (G) Macrophage population. (H) Dendritic cell population. (I) Cytokine and interleukin production analyzed using the Simpson Index of the immune response.

Optimisation of Codons for the mRNA Construct

The design of the mRNA vaccine underwent a meticulous process of codon optimisation specifically tailored to enhance compatibility with host cells. To enhance expression efficiency in human cells, the vaccine sequence was optimised

using the Java Codon Adaptation Tool (JCat) server, as illustrated in Figure 6A. The coding sequence (CDS) spans 2061 nucleotides, yielding a Codon Adaptation Index (CAI) of 0.9531 for our vaccine. In addition, the optimised construct demonstrated an average GC content of 72.44%. This comprehensive approach not only boosts the vaccine's potential

effectiveness but also highlights the critical role of codon optimisation in creating successful mRNA-based therapeutics.

Prediction of the secondary structure of the mRNA vaccine

The secondary structure of the proposed vaccine mRNA sequence was analysed using the RNAfold server, which produced a minimum free energy (MFE) score of -852.30 kcal/mol. This finding suggests that the mRNA structure is expected to maintain stability during the fabrication process. Furthermore, the proposed structure exhibits a stable central secondary configuration with a free energy of -428.78 kcal/mol. This favourable thermodynamic profile indicates that the mRNA.

Figure 6. (A) Codon optimization of the vaccine construct, yielding a Codon Adaptation Index (CAI) of 0.9531. (B) optimaized secondary structure of the vaccine mRNA; (C) centroid secondary structure of the vaccine mRNA retrieved using RNAfold server.

Prediction and validation of the secondary and tertiary structures of the translated vaccine construct

The secondary structure of the mRNA vaccine construct was analysed using the PSIPRED web server, a critical tool for assessing its folding characteristics and stability. The analysis revealed that 446 amino acids, accounting for 64.91% of the mRNA vaccine construct, were organised as random coils, making them the predominant structural feature. In contrast, alpha helices comprised 131 residues (19.06%), representing the second most common structural arrangement. The least prevalent

structure was the beta strand, consisting of 110 residues (16.01%), as illustrated in Figure 7A. To further elucidate the structural properties of the vaccine, AlphaFold 2 was employed to predict its three-dimensional (3D) conformation. This computational method generated five distinct 3D models, from which model 2 was selected based on its pLDDT score of 28.4 and pTM score of 0.141 (Figure 7B, C). Subsequently, the tertiary structure of the proposed vaccine underwent refinement through the Galaxy Refine online web server, followed by validation using a Ramachandran plot (Figure 8). The analysis revealed that 77.5% of the residues were located in the most favoured region, while 10.8%

were in the additionally allowed region, 4.9% in the generously allowed region, and 6.8% in the disallowed region. Furthermore, a negative Z-score of -2.11 obtained from ProSA-web reinforces the consistency of the 3D protein model (Figure 7D).

Collectively, these evaluations suggest that the proposed mRNA vaccine construct possesses stability, accuracy, and consistency, potentially improving its effectiveness as a vaccine candidate
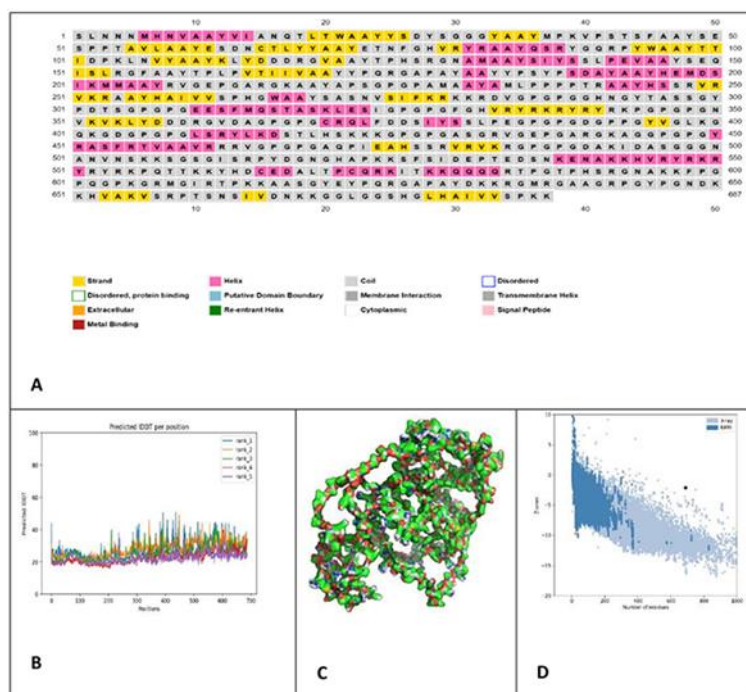

Figure 7. Prediction and validation of the structure of the peptide vaccine construct. (A) Secondary structure of the peptide vaccine construct; (B) five predicted models generated by the AlphaFold-2 server, based on predicted IDDT values per position; (C) tertiary structure of the peptide as predicted by AlphaFold-2; (D) Z-score analysis showing a Z-score of -2.11 obtained from the ProSA server.
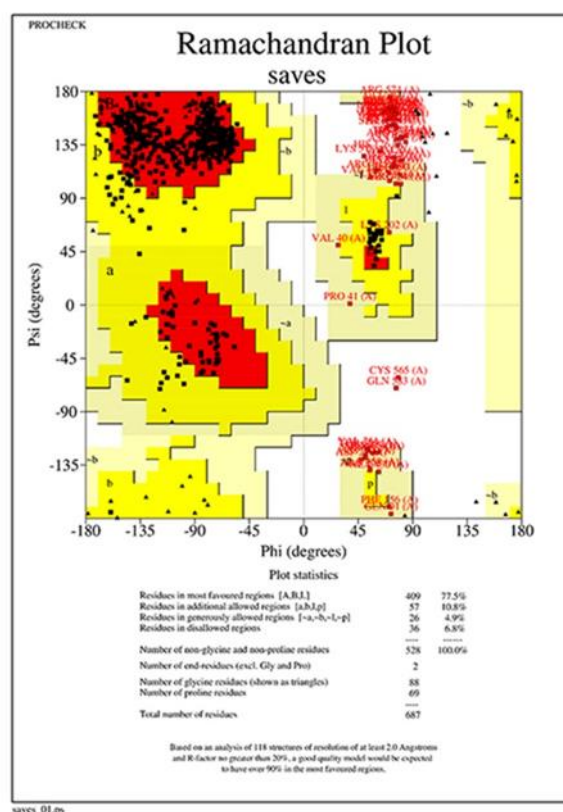
Figure 8. The Ramachandran plot, derived from the refined 3D structure of the vaccine, indicates that 77.5% of residues are located in the most favored regions.

Prediction of Conformational B-cell Epitopes

The ElliPro server was used to identify conformational B-cell epitopes based on the protein's three-dimensional folded structure. This analysis effectively detected 35 discontinuous B-cell epitopes, with prediction scores varying between 0.503 and 0.964, encompassing a total of 322 residues. Figure 9 illustrates the two-dimensional and three-dimensional models of these conformational B-cell epitopes, respectively. The identification of these epitopes is crucial for advancing vaccine design, as they can significantly enhance the immune response by promoting the generation of specific antibodies.
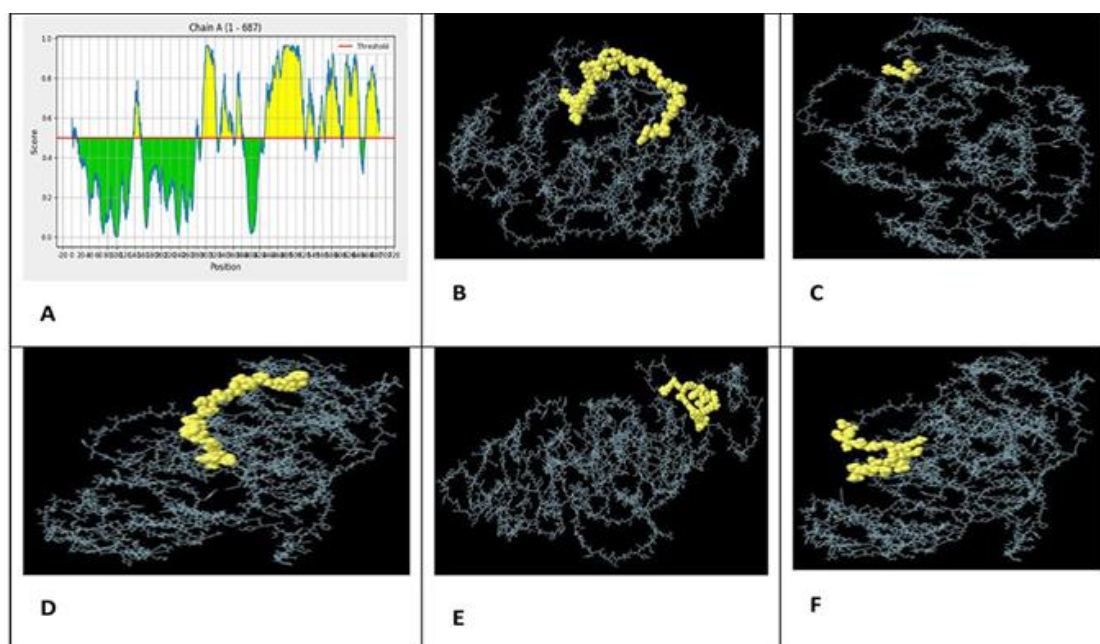
Figure 9. (A) Two-dimensional representation of the locations of studied conformational B-cell epitopes. Conformational B-cell epitopes categorized by the number of residues and their respective scores. (B) Epitope comprising 31 residues with a score of 0.918 (Rank 2). (C) Epitope consisting of 3 residues with a score of 0.964 (Rank 1). (D) Epitope containing 23 residues with a score of 0.882 (Rank 6). (E) Epitope with 16 residues and a score of 0.773 (Rank 13). (F) Epitope featuring 21 residues with a score of 0.787 (Rank 10).

Molecular docking TLRs and vaccine construct

Molecular docking studies were conducted to examine the interactions between TLR2, TLR3, TLR4, and our vaccine construct using the ClusPro server. The results reveal binding affinities of -1396.5 kcal/mol for the TLR2-vaccine construct, -1837.7 kcal/mol for the TLR3-vaccine construct, and -1460.9 kcal/mol for the TLR4-vaccine construct. The docking results were visualised using the PyMOL tool (Figure 10). Additionally, interactions between the TLRs and our vaccine candidate were analysed using the LigPlot server, as shown in Figure 10.
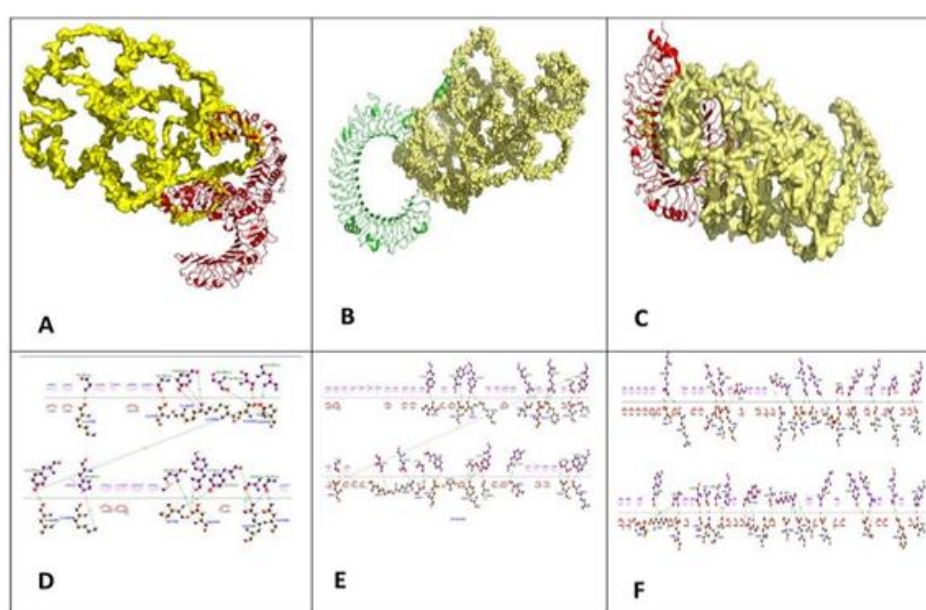
Figure 10. Docking simulations of the candidate vaccine with Toll-like receptors TLR2, TLR3, and TLR4 were conducted using the Cluspro 0.2 server, with subsequent interaction analyses performed via the LigPlot+ server. (A) Docking of the vaccine with TLR2. (B) Docking of the vaccine with TLR3. (C) Docking of the vaccine with TLR4. (D) Interaction analysis between the vaccine and TLR2. (E) Interaction analysis between the vaccine and TLR3. (F) Interaction analysis between the vaccine and TLR4.

Simulation of Molecular Dynamics

To further explore the complexes formed by the vaccine with TLR2, TLR3 and TLR4, molecular dynamics simulations were performed using the iMODS server, accompanied by an assessment of receptor-ligand interactions. the vaccine-TLR docked complexes are shown in Figs 11A, 12A and 13A. The deformability graph revealed flexible regions within the construct as prominent peaks, signifying amino acids characterized by coiled structures (Figures 11B, 12B and 13B). In addition, Normal mode analysis (NMA) was carried out to examine protein flexibility. The B-factor graphs (Figures 11D, 12D, and 13D) demonstrated the alignment between NMA findings and the PDB regions in the studied complexes The eigenvalues for the docked complexes are displayed in Figures 11F, 12F, and 13F. Overall, these results suggested that the vaccine-receptor complex displayed a low deformation index, significant rigidity, and high stability. Furthermore, the covariance matrix shown in Figures 11E, 12E, and 13E highlighted the interactions between amino acid pairs within dynamic regions. In this matrix, red signifies correlated residues, white indicates anti-correlated pairs, and blue represents non-correlated residues. Additionally, a connectivity matrix derived from the elastic network model was used to identify atom pairs connected by springs, as shown in Figures 11C, 12C, and 13C. Each chain within the complex exhibited significant stiffness, with darker grey areas representing regions of higher rigidity. These results indicate that the vaccine-receptor complex is highly stable, displaying notable rigidity and robust intermolecular interactions. Such characteristics are likely to enhance its efficacy as a vaccine against *T. canis*, providing valuable insights into its potential for inducing robust immune responses.
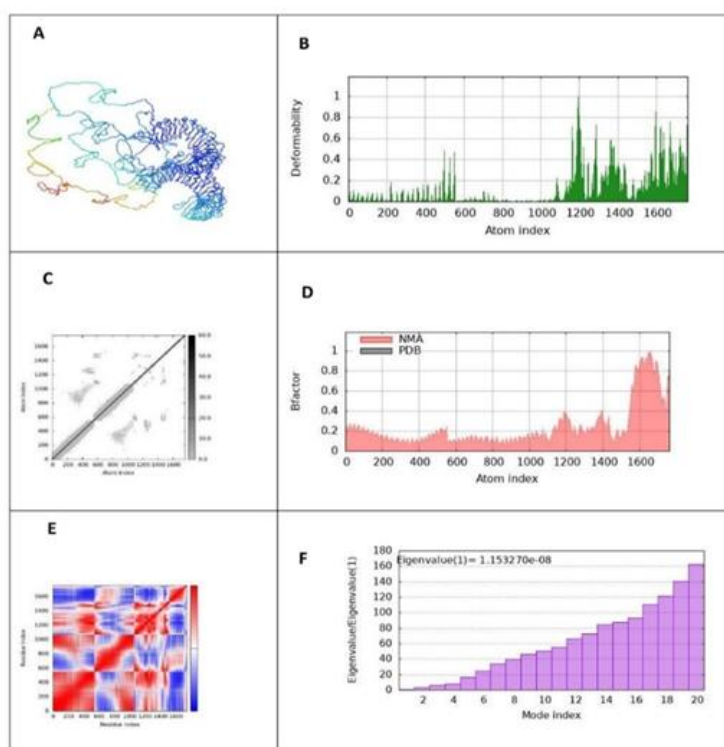

Figure 11. Molecular dynamics simulations of the docked complex of the candidate vaccine and TLR2. (A) Visualization of the vaccine-TLR2 docked complex using the iMODS server. (B) Assessment of deformability within the complex. (C) Construction of

the elastic network model utilizing the iMODS server to evaluate dynamic behavior. (D) Calculation of B-factors, indicating atomic displacement, to assess flexibility. (E) Generation of a covariance matrix to illustrate correlated movements of atomic pairs within the complex. (F) Derivation of eigenvalues to provide insights into the stability characteristics of the vaccine-TLR2 complex.
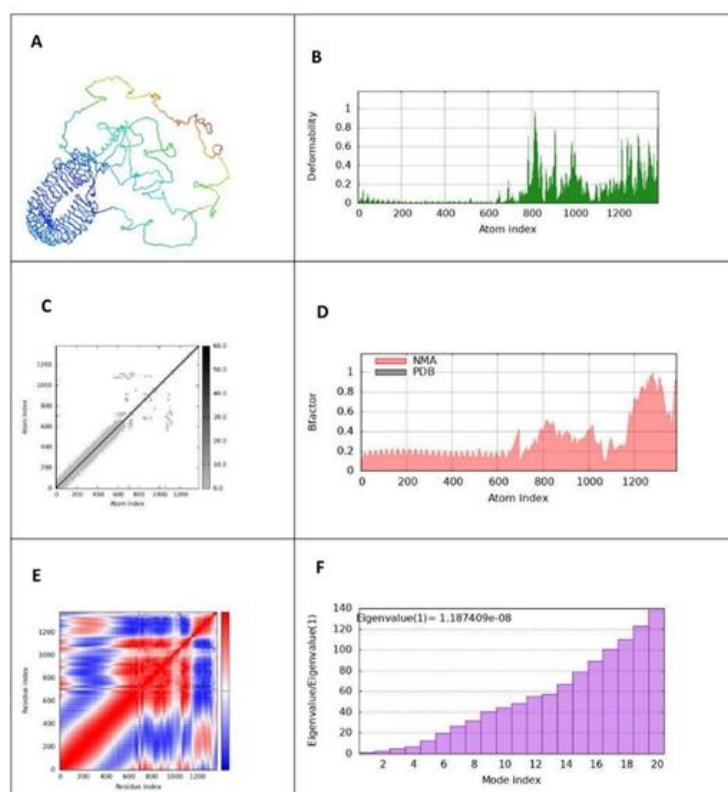

Figure 12. Molecular dynamics simulations of the docked complex of the candidate vaccine and TLR3. (A) Visualization of the vaccine-TLR2 docked complex using the iMODS server. (B) Assessment of deformability within the complex. (C) Construction of the elastic network model utilizing the iMODS server to evaluate dynamic behavior. (D) Calculation of B-factors, indicating atomic displacement, to assess flexibility. (E) Generation of a covariance matrix to illustrate correlated movements of atomic pairs within the complex. (F) Derivation of eigenvalues to provide insights into the stability characteristics of the vaccine-TLR3 complex.

Figure 13. Molecular dynamics simulations of the docked complex of the candidate vaccine and TLR4. (A) Visualization of the vaccine-TLR2 docked complex using the iMODS server. (B) Assessment of deformability within the complex. (C) Construction of the elastic network model utilizing the iMODS server to evaluate dynamic behavior. (D) Calculation of B-factors, indicating atomic displacement, to assess flexibility. (E) Generation of a covariance matrix to illustrate correlated movements of atomic pairs within the complex. (F) Derivation of eigenvalues to provide insights into the stability characteristics of the vaccine-TLR4 complex.
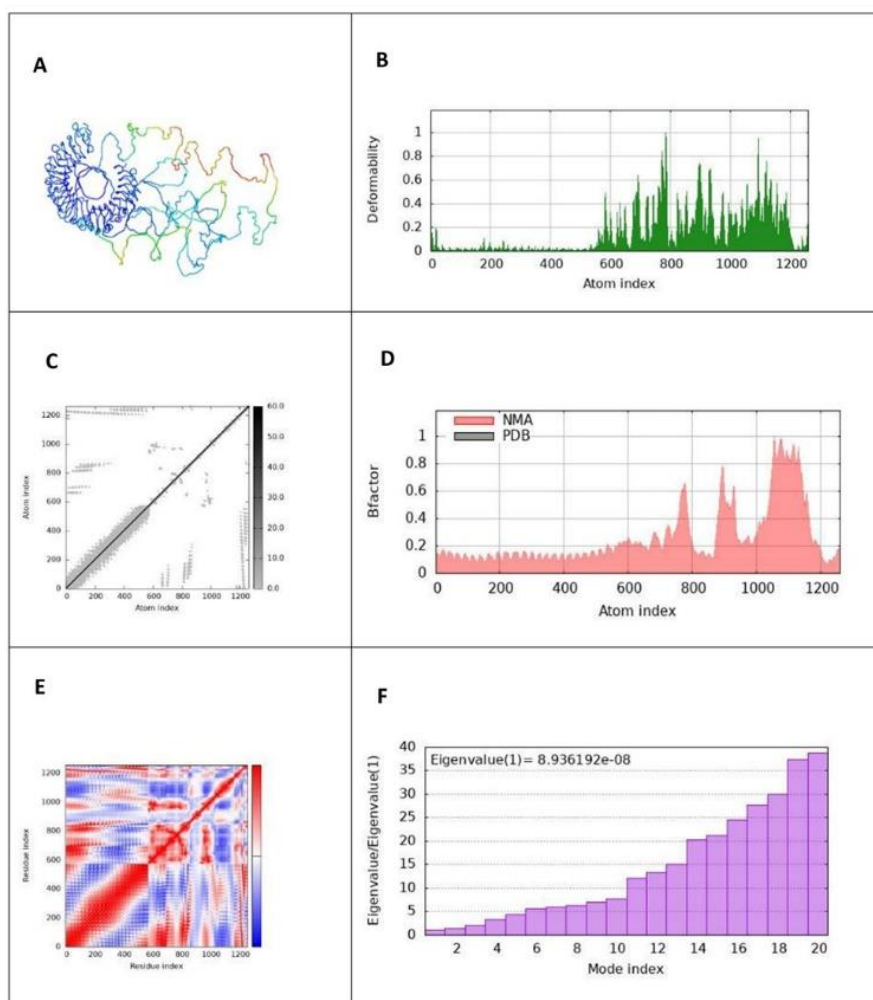
Discussion

T. canis is a notable zoonotic helminth that poses serious health risks to both humans and dogs. Although Toxocariasis is widespread, it is often underestimated across different regions, including developed and developing countries (14, 15). The main route of human infection is through contact with environments contaminated with dog faeces, especially from puppies infected with Toxocara. This situation increases the risk of human infection, particularly in children who have more frequent contact with contaminated soil or surfaces (16, 17). Prevention of this disease is based on antiparasitic drugs. This strategy provides temporary protection against infection and cannot provide lasting immunity. Therefore, the development of a vaccine to provide long-term immunological protection against *T. canis* is essential (18). Despite numerous studies conducted in the field of vaccine development against Toxocara and obtaining significant results, definitive success in developing an effective vaccine has not yet been achieved. For this reason, developing an effective vaccine against this parasite remains a major challenge. This clearly demonstrates the need for continuous review and development of innovative strategies. Continuous attention to new and creative approaches plays an important role in the progress and success of developing effective vaccines (19).

T. canis exploits several mechanisms of immune evasion to establish chronic infections in both paratenic hosts and adult dogs. The parasite secretes specific molecules that induce the proliferation and activation of regulatory T cells (Tregs). Consequently, these Tregs secrete anti-inflammatory cytokines such as IL-10 and TGF-β, which suppress host immune responses and enable chronic infection. Additional challenges, including epitope masking and parasite genetic diversity, can reduce the sensitivity of immunoassays and vaccine efficacy. These factors create significant complications in the development of accurate diagnostic methods and effective vaccines (6, 11). To overcome these challenges, our vaccine design focused on highly conserved epitopes, validated by comparing genetic data from different *T. canis* strains, to ensure robust recognition by the immune system across different parasite types.

The immune response to *T. canis* infection is mainly driven by adaptive mechanisms, particularly the activity of CD4+ T-helper type 2 (Th2) cells. These cells produce specific antibodies. The Th2 response is also accompanied by the secretion of important cytokines such as IL-4, IL-5, IL-10, and IL-13, which play an important role in regulating and controlling the immune response during infection. IL-4 promotes B-cell differentiation and antibody class switching, while IL-5 promotes eosinophil activation. These processes are important features of Toxocariasis in humans (7, 20, 22). In our study, the immune simulation performed strong induction of memory B cells and elevated antibody titres. da Silva et al. (2018) identified somatic and excretory-secretory proteins that elicited moderate antibody responses but limited activation of memory cells in mouse models. Similarly, Salazar-Garces et al. (2020) observed a 40–60% reduction in larval burden using recombinant proteins TES-30 and TMY-33, although antibody levels reduced significantly by eight weeks after immunisation. In parallel, Jaramillo-Hernandez et al. (2023) reported strong IgG1 and IgE responses but poor memory cytotoxic T cells (6, 8, 11). Our

multi-epitope mRNA vaccine may improve these limitations by long-term induction of memory B and T cells and establishing a Th1/Th2 immune balance. Although current protein-based vaccines provide partial protection, our model predicts that they will provide broader immune coverage and significantly improve the persistence of immune memory. To confirm this, these computational predictions must be validated through both in vitro and in vivo studies. Understanding these immune system dynamics is crucial for developing efficient diagnostic tools and effective therapeutic approaches against toxocariasis. A detailed understanding of these processes could greatly improve the diagnosis and control of the disease. The increasing population of feral and stray dogs increases the risk of human transmission and infection with *T. canis*. This is made more critical when there are no effective methods to remove Toxocara eggs from the environment. Consequently, the lack of such methods complicates efforts to eradicate the parasite. Preventive strategies should focus on reducing environmental contamination. These measures include regular deworming of pets, especially young animals and pregnant females, which are more susceptible to parasite transmission. Maintaining good hygiene when handling pet faeces is essential to prevent parasitic infections. Promoting good hygiene habits, such as washing hands after contact with animals, also reduces the risk of disease transmission (23-25).

Several potential vaccines have been studied to control *T. canis* infections, showing encouraging results in various trials (26). However, there are still major challenges in developing an effective vaccine for both humans and dogs. Although much progress has been made in understanding the immune responses elicited by potential vaccine candidates, there are still many challenges. These challenges include ensuring safety, proving efficacy, and triggering strong immunity in both humans and dogs. Moreover, our findings demonstrate that the multi-epitope mRNA approach can overcome some of the limitations of previous studies. These results provide

new insights into solving these challenges. Therefore, further research is needed to resolve these complexities and develop an effective vaccination strategy to reduce the impact of *T. canis* infections in human and dog populations (27).

Immunoinformatics has emerged as an advanced tool in vaccine design. It has revolutionised vaccine design by integrating computational techniques and extensive pathogen data (30). This approach makes the identification of vaccine candidates more efficient than traditional methods. Moreover, immunoinformatic methods reduce the time and resources required for vaccine development. This approach allows researchers to predict immunogenic regions and design multi-epitope vaccines (55). Such vaccines are capable of inducing robust immune responses. Despite the few immunoinformatic studies focused on *T. canis*, valuable research has been conducted by Ebrahimi et al. (2019) and Shams et al. (2021). they utilized these approaches to analyse secretory-excretory proteins for serodiagnosis purposes (12, 13). Our study builds upon this foundation by applying immunoinformatics specifically to identify epitopes from *T. canis* proteins for potential vaccine development, an area that remains underexplored compared to other pathogens. In this study, we utilized epitopes from *T. canis* proteins for the first time to predict a vaccine targeting this parasite in both humans and dogs. We extracted all protein sequences related to *T. canis* from the NCBI database, focusing on secretory proteins and those present in the cell wall due to their significant interaction with the external environment and host immune system. Using the SignalP 0.6 server, we identified proteins with signal peptides among 39,233 analysed sequences; 2,622 were found to possess signal peptides. Subsequently, we predicted their subcellular localisation using DeepLoc 2.1 and TMHMM servers. Among these proteins, 1,745 were categorised as cell wall or extracellular proteins based on their characteristics. We then identified proteins exhibiting high antigenicity using the Vaxijen v2 server, leading to a

final selection of 11 proteins, six extracellular and five cell wall proteins, that demonstrated significant potential for stimulating T and B cells in the host. From these selected proteins, we identified CTL, HTL, and LBL epitopes with high antigenicity using IEDB and ABCpred databases. To validate our vaccine candidates further, we confirmed their non-allergenic and non-toxic properties through relevant databases. To enhance structural integration among each epitope while improving functional performance, we incorporated specific linkers into our design. The selected CTL epitopes were identified through MHC-I alleles in humans and dogs; simultaneously, HTL epitopes were shown to induce important cytokines such as TNF, IL-4, IL-6, IL-10, and IL-13. Molecular docking analyses demonstrated strong binding affinities between CTL and HTL epitopes with their corresponding MHC alleles, further supporting the efficacy of our proposed vaccine construct. The mRNA construct was designed with critical elements, including a 5' m7G cap sequence, globin 5' and 3' UTRs, poly(A) tails, a Kozak sequence, and a stop codon to enhance stability and translation efficiency essential for generating strong immune responses. Additionally, binding affinity assessments with immune receptors such as TLR-2, TLR-3, and TLR-4 suggest that our vaccine construct effectively activates both innate and adaptive immune pathways, an essential factor for establishing durable immunity against *T. canis* infections. Molecular dynamics simulations have confirmed the stability of our mRNA vaccine complex, while immunoinformatics analyzes characterized it as stable, thermostable, antigenic, non-allergenic, and hydrophilic – crucial properties for practical vaccine delivery and storage applications. We anticipate that our proposed vaccine will elicit an immunological response following three doses, promoting memory cell generation necessary for long-term protection against toxocariasis. The observed activity of macrophages and dendritic cells supports our expectations regarding an effective immune response; calculations using the Simpson

Index indicate memory cell presence further corroborates this prediction.

Limitations and Strengths

This study shows an extensive in silico draft of a multi-epitope mRNA vaccine against *Toxocara canis*. Our vaccine construct demonstrated high potential to elicit robust immune responses in both humans and dogs. As a limitation, our study needs to be confirmed with experimental validation, such as in vitro or in vivo testing.

Conclusion

In conclusion, our multi-epitope mRNA vaccine showed potential as an effective strategy against *T. canis* infections. By using advanced immunoinformatic methodologies, our study represents a significant progression beyond prior research, providing a novel approach to improving protective efficacy through precisely targeted immune responses. Nevertheless, thorough validation via additional in vitro and in vivo studies is necessary to confirm its safety, immunogenicity, and overall effectiveness.

Acknowledgements

The author acknowledges the use of computational tools and publicly available data for this research.

Ethical Considerations

This study is based entirely on in silico analysis of publicly available genomic and proteomic data. Since no experiments were conducted on humans or animals, ethical approval was not necessary.

Financial Disclosure

This research received no financial support.

Competing Interests' Disclosure

The author declares no conflicts of interest.

Authors' contributions

Conceptualization, Methodology, Validation, Formal Analysis, Investigation, Resources, Software, Data Curation, Writing–Original Draft Preparation, Writing–Review & Editing, Visualization, Supervision, Project Administration: RF.

Writing Disclosure

The author utilized AI-assisted tools (DeepSeek and Perplexity) exclusively for grammatical refinement. All scientific content, analysis, and conclusions remain the author's original work.

Data Availability Statement

The data that support the findings of this study are available on request.

References

1. Chen J, Liu Q, Liu GH, Zheng WB, Hong SJ, Sugiyama H, et al. Toxocariasis: a silent threat with a progressive public health impact. Infect Dis Poverty. 2018;7(1):59. https://doi.org/10.1186/s40249-018-0437-0.

2. Menegon YA, Pinheiro NB, Santos LM, Rodrigues PRC, Avila LFC, Conceicao FR, et al. *Toxocara canis* infection may impair bovine herpesvirus type 5 immunization. Res Vet Sci. 2020;132:268–70. https://doi.org/10.1016/j.rvsc.2020.06.022.

3. Moreira GM, Telmo Pde L, Mendonca M, Moreira AN, McBride AJ, Scaini CJ, et al. Human toxocariasis: current advances in diagnostics, treatment, and interventions. Trends Parasitol. 2014;30(9):456–64. https://doi.org/10.1016/j.pt.2014.07.003.

4. Macpherson CN. The epidemiology and public health importance of toxocariasis: a zoonosis of global importance. Int J Parasitol. 2013;43(12-13):999–1008. https://doi.org/10.1016/j.ijpara.2013.07.004.

5. Smith H, Holland C, Taylor M, Magnaval JF, Schantz P, Maizels R. How common is human toxocariasis? Towards standardizing our knowledge. Trends Parasitol. 2009;25(4):182–8. https://doi.org/10.1016/j.pt.2009.01.006.

6. da Silva MB, Urrego AJ, Oviedo Y, Cooper PJ, Pacheco LGC, Pinheiro CS, et al. The somatic proteins of *Toxocara canis* larvae and excretory-secretory products revealed by proteomics. Vet Parasitol. 2018;259:25–34. https://doi.org/10.1016/j.vetpar.2018.06.015.

7. Ruiz-Manzano RA, Hernandez-Cervantes R, Del Rio-Araiza VH, Palacios-Arreola MI, Nava-Castro KE, Morales-Montor J. Immune response to chronic *Toxocara canis* infection in a mice model. Parasite Immunol. 2019;41(12):e12672. https://doi.org/10.1111/pim.12672.

8. Salazar Garces LF, Santiago LF, Santos SPO, Jaramillo Hernandez DA, da Silva MB, Alves VDS, et al. Immunogenicity and protection induced by recombinant *Toxocara canis* proteins in a murine model of toxocariasis. Vaccine. 2020;38(30):4762–72. https://doi.org/10.1016/j.vaccine.2020.04.072.

9. Maizels RM. *Toxocara canis*: molecular basis of immune recognition and evasion. Vet Parasitol. 2013;193(4):365–74. https://doi.org/10.1016/j.vetpar.2012.12.032.

10. Salama AM, Elgendy DI, Elmahy RA, Eltantawy AF, Seleem MA, Elgohary AM, et al. The potential relationship between *Toxocara canis* infection and epilepsy in a rat model. Parasitology Research. 2025;124(9):98. https://doi.org/10.1007/s00436-025-08528-7.

11. Jaramillo-Hernandez DA, Salazar Garces LF, Pacheco LGC, Pinheiro CS, Alcantara-Neves NM. Protective response mediated by immunization with recombinant proteins in a murine model of toxocariasis and canine infection by *Toxocara canis*. Vaccine. 2022;40(6):912–23. https://doi.org/10.1016/j.vaccine.2021.12.052.

12. Ebrahimi M, Seyyedtabaei SJ, Ranjbar MM, Tahvildar-biderouni F, Javadi Mamaghani A. Designing and Modeling of Multi-epitope Proteins for Diagnosis of *Toxocara canis* Infection. International Journal of Peptide Research and Therapeutics. 2020;26(3):1371–80. https://doi.org/10.1007/s10989-019-09940-1.

13. Shams M, Nourmohammadi H, Asghari A, Basati G, Majidiani H, Naserifar R, et al. Construction of a multi-epitope protein for human *Toxocara canis* detection: Immunoinformatics approach multi-epitope construct for *T. canis* serodiagnosis. Informatics in Medicine Unlocked. 2021;26:100732. https://doi.org/10.1016/j.imu.2021.100732

14. Wang N, Sieng S, Chen P, Liang T, Xu J, Han Q. Regulation Effect of *Toxocara canis* and Anthelmintics on Intestinal Microbiota Diversity and Composition in Dog. Microorganisms. 2024;12(10). https://doi.org/10.3390/microorganisms12102037.

15. Sieng S, Chen P, Wang N, Xu JY, Han Q. *Toxocara canis*-induced changes in host intestinal microbial communities. Parasit Vectors. 2023;16(1):462. https://doi.org/10.1186/s13071-023-06072-w.

16. Abe K, Shimokawa H, Kubota T, Nawa Y, Takeshita A. Myocarditis associated with visceral larva migrans due to *Toxocara canis*. Intern Med. 2002;41(9):706–8. https://doi.org/10.2169/internalmedicine.41.706.

17. Abou-El-Naga IF, Mogahed N. Potential roles of *Toxocara canis* larval excretory secretory molecules in immunomodulation and immune evasion. Acta Trop. 2023;238:106784. https://doi.org/10.1016/j.actatropica.2022.106784.

18. Mubarak AG, Mohammed ES, Elaadli H, Alzaylaee H, Hamad RS, Elkholy WA, et al. Prevalence and risk factors associated with *Toxocara canis* in dogs and humans in Egypt: A comparative approach. Vet Med Sci. 2023;9(6):2475–84. https://doi.org/10.1002/vms3.1228.

19. Ma GX, Zhou RQ, Song ZH, Zhu HH, Zhou ZY, Zeng YQ. Molecular mechanism of serine/threonine protein phosphatase 1 (PP1calpha-PP1r7) in spermatogenesis of *Toxocara canis*. Acta Trop. 2015;149:148–54. https://doi.org/10.1016/j.actatropica.2015.05.026.

20. Badri M, Ghaffarifar F, Hassan ZM, Dalimi A, Cortes H. Immunoregulatory Effects of Somatic Extract of *Toxocara canis* on Airway Inflammations in Murine Model. Iran J Parasitol. 2020;15(4):500–10. https://doi.org/10.18502/ijpa.v15i4.4855.

21. de Moura MQ, da Cunha CNO, de Sousa N, Cruz LAX, Rheingantz MG, Walcher DL, et al. Immunomodulation in the intestinal mucosa of mice supplemented with Lactobacillus rhamnosus (ATCC 7469) and infected with *Toxocara canis*. Immunobiology. 2023;228(3):152359. https://doi.org/10.1016/j.imbio.2023.152359.

22. Novak J, Machacek T, Majer M, Kostelanska M, Skulinova K, Cerny V, et al. *Toxocara canis* infection worsens the course of experimental autoimmune encephalomyelitis in mice. Parasitology. 2022;149(13):1720–8. https://doi.org/10.1017/S0031182022001238.

23. Hon LSG, Calvani NED, Ma G, Ward MP, Slapeta J. Low exposure of urban dogs in metropolitan Sydney, Australia to *Toxocara canis* demonstrated by ELISA using *T. canis* excretory-secretory (E/S) larval antigens. Vet Parasitol. 2022;302:109663. https://doi.org/10.1016/j.vetpar.2022.109663.

24. Jenkins DJ. *Toxocara canis* in Australia. Adv Parasitol. 2020;109:873–8. https://doi.org/10.1016/bs.apar.2020.01.033.

25. Rouhani-Rankouhi SZ, Kow KS, Liam CK, Lau YL. Seropositivity and risk factors of *Toxocara canis* infection in adult asthmatic patients. Trop Biomed. 2020;37(3):599–608. https://doi.org/10.47665/tb.37.3.599.

26. Mizgajska-Wiktor H, Jarosz W, Fogt-Wyrwas R, Drzewiecka A. Distribution and dynamics of soil contamination with *Toxocara canis* and Toxocara cati eggs in Poland and prevention measures proposed after 20 years of study. Vet Parasitol. 2017;234:1–9. https://doi.org/10.1016/j.vetpar.2016.12.011.

27. Ketzis JK, Lucio-Forster A. *Toxocara canis* and Toxocara cati in domestic dogs and cats in the United States, Mexico, Central America and the Caribbean: A review. Adv Parasitol. 2020;109:655–714. https://doi.org/10.1016/bs.apar.2020.01.027.

28. Teufel F, Almagro Armenteros JJ, Johansen AR, Gislason MH, Pihl SI, Tsirigos KD, et al. SignalP 6.0 predicts all five types of signal peptides using protein language models. Nat Biotechnol. 2022;40(7):1023–5. https://doi.org/10.1038/s41587-021-01156-3.

29. Odum MT, Teufel F, Thumuluri V, Almagro Armenteros JJ, Johansen AR, Winther O, et al. DeepLoc 2.1: multi-label membrane protein type prediction using protein language models. Nucleic Acids Res. 2024;52(W1):W215–W20. https://doi.org/10.1093/nar/gkae237.

30. Fattahi R, Shivaee A, Bahraminia M, Omidi N, Kalani BS. Computational design of inhibitory peptides and an mRNA-Based multi-epitope vaccine targeting the MIC3 protein of Eimeriatenella. Exp Parasitol. 2025;275:108986. https://doi.org/10.1016/j.exppara.2025.108986.

31. Saha S, Raghava GP. Prediction of continuous B-cell epitopes in an antigen using recurrent neural network. Proteins. 2006;65(1):40–8. https://doi.org/10.1002/prot.21078.

32. Andreatta M, Nielsen M. Gapped sequence alignment using artificial neural networks: application to the MHC class I system. Bioinformatics. 2016;32(4):511–7. https://doi.org/10.1093/bioinformatics/btv639.

33. Wang P, Sidney J, Kim Y, Sette A, Lund O, Nielsen M, et al. Peptide binding predictions for HLA DR, DP and DQ molecules. BMC Bioinformatics. 2010;11:568. https://doi.org/10.1186/1471-2105-11-568.

34. Sharma N, Patiyal S, Dhall A, Pande A, Arora C, Raghava GPS. AlgPred 2.0: an improved method for predicting allergenic proteins and mapping of IgE epitopes. Brief Bioinform. 2021;22(4). https://doi.org/10.1093/bib/bbaa294.

35. Sharma N, Naorem LD, Jain S, Raghava GPS. ToxinPred2: an improved method for predicting toxicity of proteins. Brief Bioinform. 2022;23(5). https://doi.org/10.1093/bib/bbac174.

36. Dhall A, Patiyal S, Raghava GPS. A hybrid method for discovering interferon-gamma inducing peptides in human and mouse. Sci Rep. 2024;14(1):26859. https://doi.org/10.1038/s41598-024-77957-8.

37. Dhanda SK, Gupta S, Vir P, Raghava GP. Prediction of IL4 inducing peptides. Clin Dev Immunol. 2013;2013:263952. https://doi.org/10.1155/2013/263952.

38. Dhall A, Patiyal S, Sharma N, Usmani SS, Raghava GPS. A Web-Based Method for the Identification of IL6-Based Immunotoxicity in Vaccine Candidates. Methods Mol Biol. 2023;2673:317–27. https://doi.org/10.1007/978-1-0716-3239-0_22.

39. Nagpal G, Usmani SS, Dhanda SK, Kaur H, Singh S, Sharma M, et al. Computer-aided designing of immunosuppressive peptides based on IL-10 inducing potential. Sci Rep. 2017;7:42851. https://doi.org/10.1038/srep42851.

40. Jain S, Dhall A, Patiyal S, Raghava GPS. IL13Pred: A method for predicting immunoregulatory cytokine IL-13 inducing peptides. Comput Biol Med. 2022;143:105297. https://doi.org/10.1016/j.compbiomed.2022.105297.

41. Guex N, Peitsch MC. SWISS-MODEL and the Swiss-PdbViewer: an environment for comparative protein modeling. Electrophoresis. 1997;18(15):2714–23. https://doi.org/10.1002/elps.1150181505.

42. Shen Y, Maupetit J, Derreumaux P, Tuffery P. Improved PEP-FOLD Approach for Peptide and Miniprotein Structure Prediction. J Chem Theory Comput. 2014;10(10):4745–58. https://doi.org/10.1021/ct500592m.

43. Asadinezhad M, Khoshnood S, Asadollahi P, Ghafourian S, Sadeghifard N, Pakzad I, et al. Development of innovative multi-epitope mRNA vaccine against Pseudomonas aeruginosa using in silico approaches. Brief Bioinform. 2023;25(1). https://doi.org/10.1093/bib/bbad502.

44. Wilkins MR, Gasteiger E, Bairoch A, Sanchez JC, Williams KL, Appel RD, et al. Protein identification and analysis tools in the ExPASy server. Methods Mol Biol. 1999;112:531–52. https://doi.org/10.1385/1-59259-584-7:531.

45. Castiglione F, Duca K, Jarrah A, Laubenbacher R, Hochberg D, Thorley-Lawson D. Simulating Epstein-Barr virus infection with C-ImmSim. Bioinformatics. 2007;23(11):1371–7. https://doi.org/10.1093/bioinformatics/btm044.

46. Grote A, Hiller K, Scheer M, Munch R, Nortemann B, Hempel DC, et al. JCat: a novel tool to adapt codon usage of a target gene to its potential expression host. Nucleic Acids Res. 2005;33(Web Server issue):W526–31. https://doi.org/10.1093/nar/gki376.

47. Sato K, Akiyama M, Sakakibara Y. RNA secondary structure prediction using deep learning with thermodynamic integration. Nat Commun. 2021;12(1):941. https://doi.org/10.1038/s41467-021-21194-4.

48. Buchan DWA, Jones DT. The PSIPRED Protein Analysis Workbench: 20 years on. Nucleic Acids Res. 2019;47(W1):W402–W7. https://doi.org/10.1093/nar/gkz297.

49. Wroblewski K, Kmiecik S. Integrating AlphaFold pLDDT Scores into CABS-flex for enhanced protein flexibility simulations. Comput Struct Biotechnol J. 2024;23:4350–6. https://doi.org/10.1016/j.csbj.2024.11.047.

50. Wiederstein M, Sippl MJ. ProSA-web: interactive web service for the recognition of errors in three-dimensional structures of proteins. Nucleic Acids Res. 2007;35(Web Server issue):W407–10. https://doi.org/10.1093/nar/gkm290.

51. Laskowski RA, Rullmannn JA, MacArthur MW, Kaptein R, Thornton JM. AQUA and PROCHECK-NMR: programs for checking the quality of protein structures solved by NMR. J Biomol NMR. 1996;8(4):477–86. https://doi.org/10.1007/BF00228148.

52. Ponomarenko J, Bui HH, Li W, Fusseder N, Bourne PE, Sette A, et al. ElliPro: a new structure-based tool for the prediction of antibody epitopes. BMC Bioinformatics. 2008;9:514. https://doi.org/10.1186/1471-2105-9-514.

53. Laskowski RA, Swindells MB. LigPlot+: multiple ligand-protein interaction diagrams for drug discovery. J Chem Inf Model. 2011;51(10):2778–86. 10.1021/ci200227u.

54. Lopez-Blanco JR, Aliaga JI, Quintana-Orti ES, Chacon P. iMODS: internal coordinates normal mode analysis server. Nucleic Acids Res. 2014;42(Web Server issue):W271–6. https://doi.org/10.1093/nar/gku339.

55. Fattahi R, Sadeghi Kalani B. mRNA vaccine design using the proteome of Theileria annulata through immunoinformatics approaches. mSphere. 2025;10(5):e0080924. https://doi.org/10.1128/msphere.00809-24.